Refining Ephemeris and Estimating Period Change Rate for V965 Cephei

Maksym Pyatnytskyy
Dzhona Makkeina 37, apt. 6, Kyiv, 01042, Ukraine; mpyat2@gmail.com

Received December 13, 2020; revised February 2, March 19, 2021; accepted March 30, 2021

Abstract Using observations from the AAVSO International Database, data from the literature, and new photometry from the current investigation, the author has produced an O–C diagram for the HADS star V965 Cephei for the time interval September 2011 through December 2020. Analysis of the O–C diagram revealed that V965 Cep has been increasing its period at a constant rate $(1/P)(dP/dt)$ of $1.02(8)\times10^{-6}$ yr^{-1}. A refined ephemeris for the star: $T_{max}(HJD) = 2457504.8963(2) + 0.085067421(9)\,E + 1.01(8)\times10^{-11}\,E^2$.

1. Introduction

The variable star NSVS 304708 (later named V965 Cephei) appeared in a table entry from the Northern Sky Variability Survey by J. Scott Shaw and collaborators (provided by Wozniak *et al.* 2004). The star was originally classified as a W Ursae Majoris-type (EW) eclipsing variable. Based on the shape of its light curve and period that is shorter than typical periods of eclipsing EW-type stars, Sokolovsky (2009) reclassified it as a High Amplitude δ Scuti (HADS) pulsating star with one dominant pulsation with a period of 0.0850695 (0.000002) d. At the time of writing, the AAVSO VSX database (Watson *et al.* 2014) showed this period for V965 Cep.

Analyzing his observational data along with data from the AAVSO International Database, the author found that the folded light curve built using the period from the VSX looked "messy." This indicated that the VSX period was not consistent with the observations during September 2011–December 2020, either due to the period's inaccuracy or because the period has changed over time.

Many HADS stars (including their superclass, δ Scuti stars) exhibit period changes. These changes could be caused by stellar evolution, the presence of an undiscovered companion, i. e., light-time effect, secular changes in the chemical structure, nonlinear interactions between pulsation modes (Breger and Pamyatnykh 1998; Templeton 2005; Sterken 2005; Neilson and Percy 2016). This paper investigates the behavior of the HADS V965 Cephei during the past decade.

2. Methods

An effective commonly used method for diagnostic variation of the period is analyzing a dependency of observed minus calculated (O–C) times of maxima on a number of a variability cycle (Sterken 2005). An O–C diagram was utilized in the current work to analyze the suspected period change.

The analysis drew on published times of maxima for V965 Cep (Wills *et al.* 2012, 2013, 2014, 2015) and an ample number of V965 Cep observations available through the AAVSO International Database for September 2011–November 2020.

The author also observed V965 Cep during two nights in December 2020 using a 6-inch f/5 Newtonian with ZWO ASI120MM-S CMOS camera with a photometric V filter. The observational site was in a relatively highly light-polluted urban area (Osokorky neighborhood, Kyiv, Ukraine). The author used his toolkit (Pyatnytskyy 2018–2020) to calibrate images. The differential aperture photometry was performed with AstroImageJ (Collins *et al.* 2017). Table 1 lists comparison and check stars from a standard AAVSO sequence. Standardized magnitudes were transformed using one-band transformation with the Tv_b-v transformation coefficient obtained from photometry of the AAVSO Standard Field for M67 and with the target's (B–V) index (0.44) from the VSX. The Tv_b-v value turned out to be relatively small (0.0086 (0.0042)); therefore, the transformation introduced a minor correction to the data. The observations can be found in the AAVSO database by observer code PMAK.

The initial analysis of the light curve was carried out with VStar software (Benn 2013). The Date Compensated Discrete Fourier Transform (DC DFT) was performed on data in the Johnson V filter available from the AAVSO International Database and data from The All-Sky Automated Survey for Supernovae (ASAS-SN) (Kochanek *et al.* 2017). The power spectrum of the light curve for V965 Cep showed only one dominant frequency corresponding to a period of 0.0850674 d (Figure 1). Other prominent peaks seen in the plot in Figure 1 are alias frequencies separated by a 1-day interval. The peak at a frequency of 1 day^{-1} is a "phantom" caused by gaps in the source data; the rightmost peak with a period of 0.0425337 d corresponds to the second harmonic.

Knowing the period's crude value, we can determine exact times of maxima in the AAVSO data using an approach described by Wils *et al.* (2009). Since only one dominant frequency exists, the light curve shape should reoccur in each pulsation cycle; thus, we can create an average light curve

Table 1. Comparison and check stars.

AAVSO UID	*Type*	*R. A. (2000)* h m s	*Dec. (2000)* ° ′ ″	*B*	*V*	*B-V*
000-BMX-931	Comparison	00 08 27.43	80 20 25.3	13.986	13.038	0.948
000-BMX-933	Check	00 12 28.41	80 14 29.5	14.495	13.783	0.712

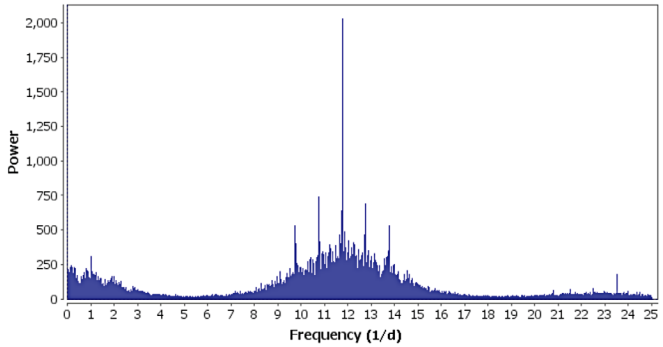

Figure 1. Power spectrum of the light curve for V965 Cep in the V band. The light curve includes data from the AAVSO International Database (September 2011–November 2020), the author's observations (December 2020), and ASAS-SN data (January 2014–November 2018). The primary peak corresponds to a period of 0.0850674 d.

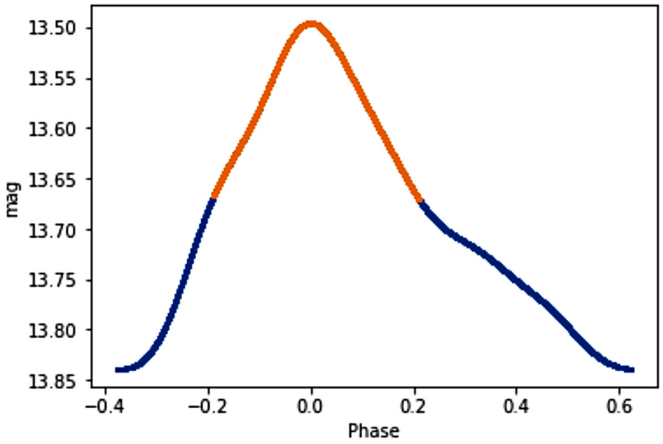

Figure 2. The average cycle profile for V965 Cep. The part of the profile used for light curve matching to determine times of maximum light is shown in the lighter color.

profile for a cycle. Shifting this average profile along the time and magnitude axes near a particular maximum (shift along magnitude axis is required to compensate systematic magnitude offsets for different observers), matches with the observed light curve can then be found, with the best match corresponding to the precise time of maximum.

To create the average cycle profile, a VSTAR-built Fourier model was used, i. e., approximation of the light curve (observations from AAVSO) with a trigonometric polynomial composed of the primary frequency and its harmonics (up to the 6th harmonic). Figure 2 shows the resulting average cycle profile.

For practical purposes, the upper part of this model profile was taken, from the highest point (maximum) to half-height (see Figure 2). Shifting this partial profile by time and magnitude around the selected maximum and applying the least-squares procedure to the measured and calculated magnitudes, a required value of time of the maximum was obtained; the procedure was repeated for each maximum seen in the data. Figure 3 shows typical results of light curve matching. Even when the observations were incomplete, a position of the maximum was estimated well.

Measurement uncertainty of a particular time of maximum was estimated by calculating a square root of the average

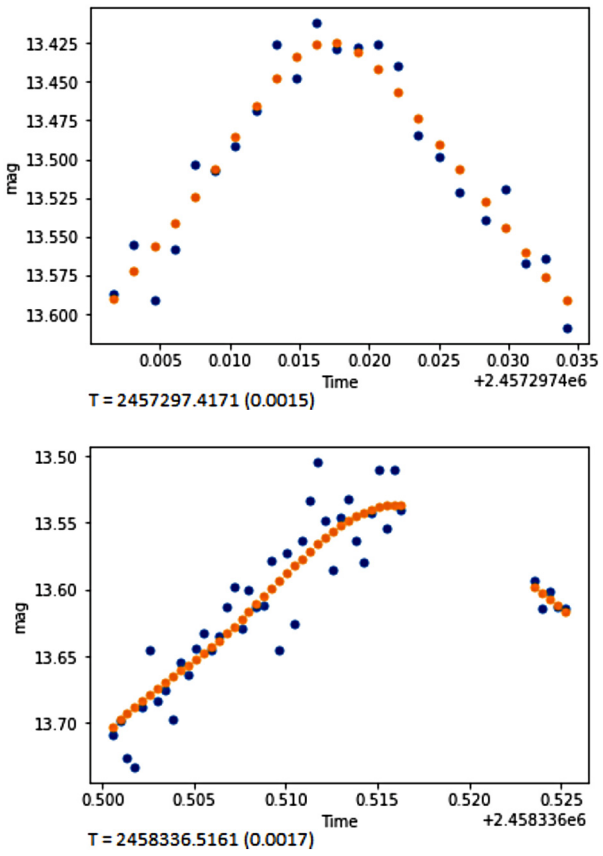

Figure 3. Examples of light curve matching. Observed values are indicated by the dark points and the modeled light curve is shown in a lighter color.

squared difference in time between observations and the matched profile (according to Wils *et al.* 2009). The light curve matching was performed using a PYTHON tool developed by the author.

3. Results and discussion

Table 2 lists the times of maxima. Most maxima found in the literature (Wills *et al.* 2012, 2013, 2014, 2015) could also be derived from the AAVSO data; those maxima were associated with the same observers as in the mentioned papers. For maxima from the AAVSO dataset, the author used his estimations for maxima times rather than those available in other sources. Figure 4 presents the O–C diagram built based on times of maxima listed in Table 2.

Zero epoch (zero cycle) was chosen as a mean time between the first and the last times of maxima available. The zero epoch period P_0 was initially set to the value obtained by DC DFT and improved at the next step (see below). The O–C diagram shows that the period does change over time. Assuming that the change rate is constant, we can approximate the points by the quadratic function:

$$O–C = T_{max} – (T_0 + P_0 E) = \alpha E + 0.5 \beta E^2 + const \quad (1)$$

where T_{max} is the observed time of a maximum, E is its epoch (the cycle number of this maximum), T_0 is the time of the zero epoch, and β is a period change rate. The value of P_0 was

Table 2. Times of maxima, epochs, and O-C values.

Maximum	*Time of Maximum (HJD)*	*Uncertainty (d)*	*Epoch (Cycle Number)*	*O–C (d)*	*Source*	*AAVSO Observer Code*
1	2455836.3027	0.0019	–19615	0.0038	Wils *et al.* 2012	—
2	2455836.3869	0.0010	–19614	0.0030	Wils *et al.* 2012	—
3	2456886.3727	0.0019	–7271	0.0016	Wils *et al.* 2015	—
4	2455818.3536	0.0040	–19826	0.0040	AAVSO	VMAE
5	2455818.4396	0.0026	–19825	0.0049	AAVSO	VMAE
6	2456110.4736	0.0025	–16392	0.0024	AAVSO	VMAE
7	2456110.5591	0.0027	–16391	0.0029	AAVSO	VMAE
8	2456134.4620	0.0015	–16110	0.0018	AAVSO	VMAE
9	2456134.5485	0.0013	–16109	0.0032	AAVSO	VMAE
10	2456135.3988	0.0025	–16099	0.0029	AAVSO	VMAE
11	2456135.4826	0.0030	–16098	0.0017	AAVSO	VMAE
12	2456223.3587	0.0022	–15065	0.0030	AAVSO	VMAE
13	2456496.4227	0.0021	–11855	0.0006	AAVSO	VMAE
14	2456628.4463	0.0017	–10303	–0.0004	AAVSO	PNQ
15	2456628.5335	0.0022	–10302	0.0017	AAVSO	PNQ
16	2456733.3361	0.0017	–9070	0.0013	AAVSO	VWS
17	2456853.5379	0.0026	–7657	0.0029	AAVSO	VMAE
18	2456855.4921	0.0029	–7634	0.0005	AAVSO	VMAE
19	2456913.3383	0.0021	–6954	0.0008	AAVSO	VMAE
20	2456913.4237	0.0027	–6953	0.0012	AAVSO	VMAE
21	2456913.5079	0.0022	–6952	0.0003	AAVSO	VMAE
22	2457283.3794	0.0019	–2604	–0.0013	AAVSO	VMAE
23	2457283.4643	0.0018	–2603	–0.0015	AAVSO	VMAE
24	2457297.3316	0.0012	–2440	–0.0002	AAVSO	VMAE
25	2457297.4171	0.0015	–2439	0.0002	AAVSO	VMAE
26	2457614.4633	0.0014	1288	0.0001	AAVSO	VWS
27	2457618.3761	0.0009	1334	–0.0002	AAVSO	VMAE
28	2457618.4615	0.0009	1335	0.0002	AAVSO	VMAE
29	2457618.5472	0.0012	1336	0.0008	AAVSO	VMAE
30	2457623.3959	0.0007	1393	0.0006	AAVSO	VMAE
31	2457623.4809	0.0008	1394	0.0005	AAVSO	VMAE
32	2457623.5649	0.0009	1395	–0.0004	AAVSO	VMAE
33	2457633.3479	0.0007	1510	–0.0003	AAVSO	VMAE
34	2457633.4326	0.0008	1511	–0.0006	AAVSO	VMAE
35	2457633.5191	0.0014	1512	0.0009	AAVSO	VMAE
36	2457641.4288	0.0015	1605	–0.0007	AAVSO	VWS
37	2458020.3191	0.0007	6059	–0.0007	AAVSO	VMAE
38	2458020.4054	0.0008	6060	0.0005	AAVSO	VMAE
39	2458020.4903	0.0014	6061	0.0004	AAVSO	VMAE
40	2458336.4302	0.0026	9775	–0.0002	AAVSO	VWS
41	2458336.5161	0.0017	9776	0.0007	AAVSO	VWS
42	2458390.6204	0.0012	10412	0.0021	AAVSO	DFS
43	2458390.7055	0.0016	10413	0.0021	AAVSO	DFS
44	2458541.3605	0.0013	12184	0.0027	AAVSO	SDWA
45	2458541.4447	0.0011	12185	0.0018	AAVSO	SDWA
46	2458541.5289	0.0014	12186	0.0010	AAVSO	SDWA
47	2458646.5029	0.0013	13420	0.0018	AAVSO	DFS
48	2458680.5294	0.0014	13820	0.0013	AAVSO	DFS
49	2458680.6145	0.0012	13821	0.0014	AAVSO	DFS
50	2458716.4278	0.0015	14242	0.0012	AAVSO	VWS
51	2458734.6334	0.0009	14456	0.0025	AAVSO	DFS
52	2458764.5771	0.0010	14808	0.0024	AAVSO	DFS
53	2458764.6624	0.0017	14809	0.0026	AAVSO	DFS
54	2458877.2900	0.0010	16133	0.0009	AAVSO	SDWA
55	2458877.3756	0.0010	16134	0.0015	AAVSO	SDWA
56	2459036.5411	0.0024	18005	0.0058	AAVSO	DFS
57	2459036.6250	0.0019	18006	0.0047	AAVSO	DFS
58	2459066.5693	0.0016	18358	0.0053	AAVSO	DFS
59	2459156.4002	0.0015	19414	0.0050	AAVSO	SDWA
60	2459156.4835	0.0019	19415	0.0032	AAVSO	SDWA
61	2459190.2551	0.0021	19812	0.0030	AAVSO	PMAK
62	2459190.3397	0.0022	19813	0.0026	AAVSO	PMAK
63	2459191.1924	0.0022	19823	0.0045	AAVSO	PMAK
64	2459191.2757	0.0024	19824	0.0029	AAVSO	PMAK
65	2459191.3616	0.0032	19825	0.0037	AAVSO	PMAK

chosen so that the minimum of the approximating parabola coincides with zero epoch (i.e., α becomes null). The fitting of the quadratic function to O–C data and tuning of P_0 was performed using LibreOffice Calc. The best fit delivered the following equation for the ephemeris:

$$T_{max}(HJD) = 2457504.8963(2) + 0.085067421(9)\,E + 1.01(8)\times10^{-11}\,E^2 \quad (2)$$

The period change rate is $2.03(17)\times10^{-11}$ days/cycle, which corresponds to the rate of $(1/P)(dP/dt)\,1.02(8)\times10^{-6}\,yr^{-1}$.

Figure 5 shows the folded light curve with AAVSO and ASAS-SN data in V-filter built using the obtained period and epoch. For AAVSO data, zero magnitude levels for each cycle were adjusted based on the profile fitting outcomes.

The obtained value of $1.02(8)\times10^{-6}\,y^{-1}$ for $(1/P)(dP/dt)$ is relatively high. Breger and Pamyatnykh (1998) give a characteristic value of $(1/P)(dP/dt)$ for δ Scuti stars around 10^{-7} year^{-1} (with equal distribution between positive and negative values); they hold that even such values cannot be fully explained by stellar evolution. In their sample, only stars with nonradial pulsations have absolute values of $(1/P)(dP/dt)$ that are close to or greater than $1\times10^{-6}\,yr^{-1}$. For such multiperiodic stars, a cause of period change might be nonlinear mode-coupling (Breger and Pamyatnykh 1998; Templeton 2005). However, V965 Cep is a high amplitude δ Scuti star that oscillates at one frequency (see Figure 1); therefore, it looks like a radial-mode pulsator (Templeton 2005). Another possible cause of the period change is a light-time effect in binary systems (Sterken 2005; Templeton 2005). However, there is no evidence that V965 Cep belongs to such a system (Liakos and Niarchos 2017).

To prove the effect and rule out any observation bias, an independent set of observations was used, namely, a quite long yet sparse ASAS-SN series (Kochanek *et al.* 2017). Two intervals were taken: from JD 2456681 to JD 2458028 (data in V band) and from JD 2458033 to JD 2459167 (data in g band). DC DFT performed on each subset returned a period of 0.08506731 d for the first subset (V band, mean JD = 2457241) and 0.08506771 d for the second subset (g band, mean JD = 2458612). A difference in periods for these two intervals is 4×10^{-7} d, and a difference in mean epochs is 1,372 days. From those values, we can derive a crude estimation of the period change rate as $\sim1.3\times10^{-6}\,yr^{-1}$, which is consistent with the value of $(1/P)(dP/dt)$ obtained from O–C diagram. Its unusually high rate of period change makes V965 Cep an interesting object that deserves continuing observations.

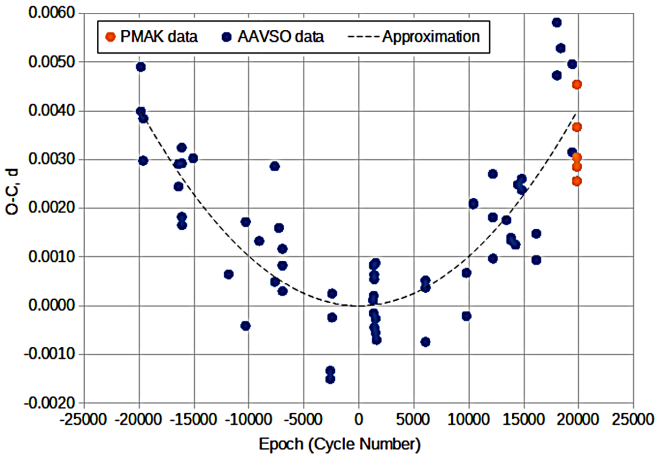

Figure 4. O–C diagram for V956 Cep (T_0 = HJD 2457504.8963, P_0 = 0.085067421 d). Maxima derived from the author's observations (observer code PMAK in Table 2) are indicated by the lighter points. The dashed line is the approximating quadratic function.

4. Conclusions

Analysis of the O–C diagram for a high amplitude delta Scuti star V965 Cep showed that the star exhibits period change for the past decade. From September 2011 to December 2020, its period has been growing with a constant rate of $2.03(17)\times10^{-11}$ days/cycle, which corresponds to $(1/P)(dP/dt)$ of $1.02(8)\times10^{-6}\,yr^{-1}$. The period for the epoch HJD 2457504.8963 was 0.085067421 d.

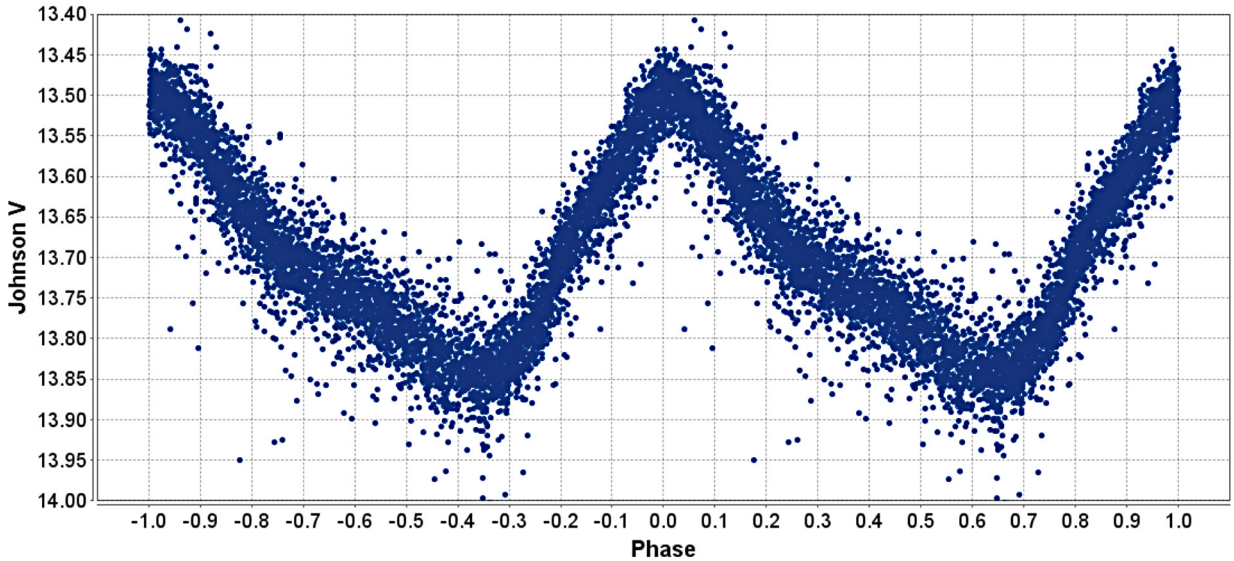

Figure 5. The folded light curve with AAVSO and ASAS-SN data. Magnitude zero levels for AAVSO data corrected for each cycle.

5. Acknowledgements

This research was made possible through the use of variable star observations from the AAVSO International Database (AAVSO 2013) and respective valuable contributions by observers DFS, PNQ, SDWA, VMAE, VWS. It also benefitted from the use of the International Variable Star Index (VSX) database operated at AAVSO, Cambridge, Massachusetts, USA.

References

AAVSO. 2013, Observations from the AAVSO International Database (http://www.aavso.org).

Benn, D. 2013, VSTAR data analysis software (https://www.aavso.org/vstar-overview).

Breger, M, and Pamyatnykh, A. A. 1998, *Astron. Astrophys.*, **332**, 958.

Collins, K. A., Kielkopf, J. F., Stassun, K. G., and Hessman, F. V. 2017, *Astron. J.*, **153**, 77.

Kochanek, C. S., *et al.* 2017, *Publ. Astron. Soc. Pacific*, **129**, 104502.

Liakos, A., and Niarchos, P. 2017, *Mon. Not. Roy. Astron. Soc.*, **465**, 1181.

Neilson, R. N., and Percy J. R. 2016, *J Amer. Assoc. Var. Star Obs.*, **44**, 179.

Pyatnytskyy, M. Yu. 2018–2020, FITS Command-line Utilities (http://fits-command-line-utilities.sourceforge.net).

Sokolovsky, K. V., 2009, *Perem. Zvezdy Prilozh.*, **9**, 30.

Sterken, C., ed. 2005, The Light-Time Effect in Astrophysics: Causes and Cures of the O–C Diagram, ASP Conf. Ser., 335, Astronomical Society of the Pacific, San Francisco.

Templeton, M. R. 2005, *J Amer. Assoc. Var. Star Obs.*, **34**, 1

Watson, C., Henden, A. A., and Price, C. A. 2014, AAVSO International Variable Star Index (VSX, Watson+, 2005-2014, https://www.aavso.org/vsx).

Wils P., *et al.* 2009, *Inf. Bur. Var. Stars*, No. 5878, 1.

Wils P., *et al.* 2012, *Inf. Bur. Var. Stars*, No. 6015, 1.

Wils P., *et al.* 2013, *Inf. Bur. Var. Stars*, No. 6049, 1.

Wils P., *et al.* 2014, *Inf. Bur. Var. Stars*, No. 6122, 1.

Wils P., *et al.* 2015, *Inf. Bur. Var. Stars*, No. 6150, 1.

Woźniak, P. R., *et al.* 2004, *Astron. J.*, 127, 2436 (https://www.physast.uga.edu/~jss/nsvs/).